

Heavy-flavor production in dense QCD matter

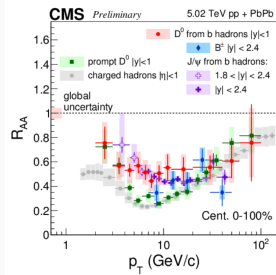
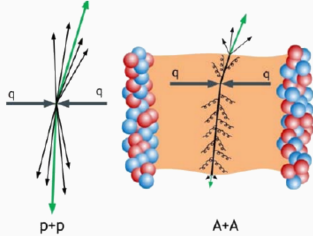
*The 29th International Workshop on Deep-Inelastic Scattering & Related Subjects
Santiago de Compostela, Spain, May 02-06, 2022*

Weiyao Ke and Ivan Vitev, Los Alamos National Laboratory

arXiv:2204.00634, submitted to PRC

May 04, 2022 (online)

Heavy flavor production in p - p and A - A



$$R_{AA} = \frac{dN_{AA \rightarrow h}/dp_T}{\langle T_{AA} \rangle d\sigma_{pp \rightarrow h}/dp_T}$$

- Factorized formula for charm & bottom meson production

$$d\sigma_{pp \rightarrow h} = f_{i/p}(x_i, Q) f_{j/p}(x_j, Q) \otimes d\hat{\sigma}_{ij \rightarrow k} \otimes D_{h/k}(z, \mu_F)$$

- In A - A , QCD medium introduces additional scales
 - Cold nuclear matter (CNM): $\Delta k_T^2 \sim \Lambda^2(A^{1/3} - 1)$.
 - Quark-gluon plasma (QGP): $T, \mu_D \sim g_s T$.

- Modified heavy-flavor production in A - A

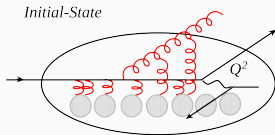
- Initial states: $f_{i/p} f_{j/p} \rightarrow f_{i/A} f_{j/B}(x; \Delta k_T^2, \dots)$.
- Final states: $D(z) \rightarrow D_{\text{med}}(z; T \dots)$.

- Mass is additional handle to probe medium properties.

A study of light & heavy with both IS and FS effects.

Initial-state effects I: multiple collisions

In p -A collisions ▽

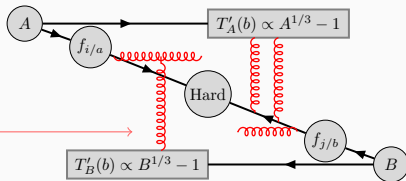


- Multiple collisions lead to transverse momentum broadening (Cronin effect)

$$\langle k_{\perp}^2 \rangle = 2\mu^2 \xi \frac{L}{\lambda_{q,g}}$$

$$\mu^2 = 0.12 \text{ GeV}^2, \quad 1.0 < \lambda_g < 1.5 \text{ fm.}$$

Generalization to A-A collisions ▽



Multiple collision broadening
and power corrections

- Power corrections from coherent multiple collisions (dynamical shadowing) [J.-W. Qiu, I. Vitev, PLB632 507-511], effectively shift parton momentum fractions by

$$\frac{\delta x_a}{x_a} \propto \frac{\langle k_{\perp}^2 \rangle_B}{-u}, \quad \frac{\delta x_b}{x_b} \propto \frac{\langle k_{\perp}^2 \rangle_A}{-t}$$

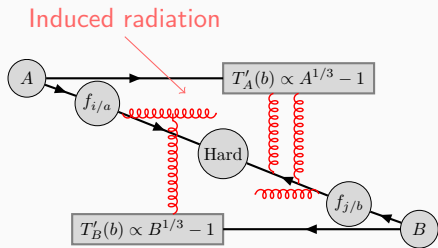
$$f(x, \mu) \rightarrow f(x + \delta x, \mu) \frac{1}{\pi} e^{-k_{\perp}^2 / \langle k_{\perp}^2 \rangle}$$

Initial-state effects II: radiative energy loss in the CNM

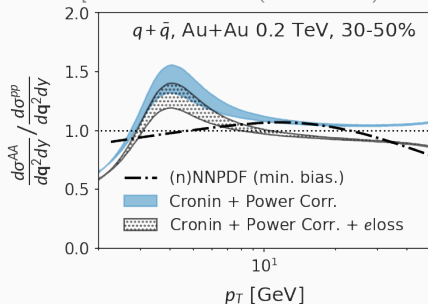
Energy loss from medium-induced initial-state soft gluon emissions [I. Vitev, PRC75(2007)064906]

$$\frac{\Delta x_a}{x_a} \approx \frac{L_B}{\lambda_g} \int_{m_N/p^+}^1 dx \int_{(xm_N)^2}^{(xp^+)^2} dk_{\perp}^2 \frac{\alpha_s C_R}{\pi} \int_0^{\frac{\mu p^+}{4}} d^2 q_{\perp} \frac{\mu^2}{\pi(q_{\perp}^2 + \mu^2)^2} \left[\frac{q_{\perp}^2}{k_{\perp}^2 (k_{\perp} - q_{\perp})^2} - \frac{2(q_{\perp}^2 - q_{\perp} \cdot k_{\perp})}{k_{\perp}^2 (k_{\perp} - q_{\perp})^2} \frac{\sin \frac{k_{\perp}^2 L_B}{xp^+}}{\frac{k_{\perp}^2 L_B}{xp^+}} \right]$$

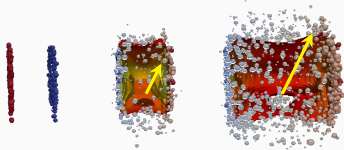
Broadening + power corr. + e loss: $f(x, \mu) \rightarrow f(x + \delta x + \Delta x, \mu) \frac{1}{\pi} e^{-k_{\perp}^2 / \langle k_{\perp}^2 \rangle}$



▽ Dynamical approach [Z.-B. Kang et al. PLB718(2012)482-487]
v.s. nNNPDF [R. A. Khalek et al. (nNNPDF3.0) 2201.12363.]



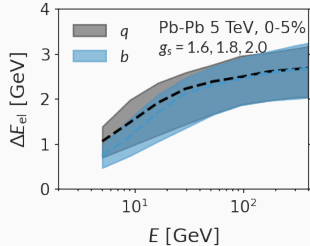
Final-state effects I: elastic energy loss in the quark-gluon plasma



Hydrodynamic-based simulation of QGP provides temperature profiles $T(\tau, x, y)$

[H. Song, U. Heinz, PRC77(2008)064901;

J. E. Bernhard, 1804.06469;]



- HTL collisional energy loss of hard parton [E. Braaten, M. H. Thoma PRD44(1991)R2625(R).] :

$$\Delta E_{\text{el}} = \int_{x_0}^{x_0 + \hat{n} \Delta z} d\Delta z \frac{C_R}{4} \mu_D^2 \alpha_s(ET) \ln \left(\frac{ET}{\mu_D^2} \right) \left(\frac{1}{v} - \frac{1-v^2}{2v^2} \ln \frac{1+v}{1-v} \right)$$

Screening (Debye) mass in the QGP: $\mu_D = \sqrt{1 + \frac{N_f}{6} g_s} T$.

- As an approximation, we use an event-averaged $\langle \Delta E_{\text{el}} \rangle$ to shift the final-state parton momentum in the perturbative cross-section (NLO)

$$d\sigma_{AA \rightarrow h} = f_{i/p} f_{j/p} \otimes d\hat{\sigma}_{ij \rightarrow k}(E + \langle \Delta E_{\text{el}} \rangle) \otimes D_{h/k}(z, \mu_F)$$

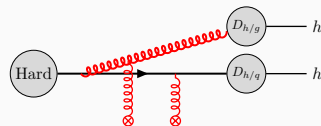
Medium-modified splitting functions from SCET_G

- SCET_G: SCET Lagrangian coupled to background Glauber gluon of the medium[G.

Ovanesyan, I. Vitev, JHEP06(2011)080

$$\mathcal{L}_{\text{SCET}}(\xi_n, A_n) + \mathcal{L}_G(\xi_n, A_n, A_G)$$

$$\mathcal{L}_G = e^{-i(p-p')x} \left[\bar{\xi}_n \Gamma_{qqG}^{\mu,c} \xi_n - i \Gamma_{ggG}^{\mu\alpha\beta,cab} A_{n,\alpha}^a A_{n,\beta}^b \right] A_{G,\mu}^c(x)$$



- Background A_G is a superposition of the color field generate by medium sources,

$$A^{\mu,a}(x) = \sum_i g_s \int e^{-iq(x-y)} \frac{g^{\mu\nu} + \dots}{q^2 - \mu_D^2} J_{\nu,i}^a(y) dy^4, \quad q \sim (\lambda^2, \lambda^2, \vec{\lambda})$$

- Here source is assumed to be static ($J^i = 0, J^0 \neq 0$), with the local densities $\langle J^0(x) \rangle = \frac{d_{q,g}}{e^{p \cdot u(x)/T(x)} \pm 1}$ for quarks and gluons

Medium-modified splitting functions from SCET_G

- Medium-modified splitting functions for heavy quark [Kang, Ringer, Vitev, JHEP03(2017)146] :

$\nabla \Delta P_{QQ}$

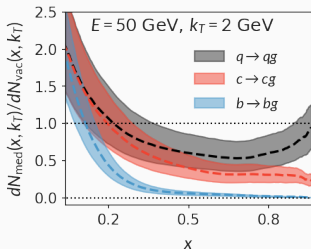
$\Delta P_{Qg} \triangleright$

$$\begin{aligned} \left(\frac{dN^{\text{med}}}{dx d^2k_{\perp}} \right)_{Q \rightarrow Qg} &= \frac{\alpha_s}{2\pi^2} C_F \int \frac{d\Delta z}{\lambda_g(z)} \int d^2q_{\perp} \frac{1}{\sigma_{\text{el}}} \frac{d\sigma_{\text{el}}^{\text{med}}}{d^2q_{\perp}} \left\{ \left(\frac{1+(1-x)^2}{x} \right) \left[\frac{B_{\perp}}{B_{\perp}^2 + \nu^2} \right. \right. \\ &\times \left(\frac{B_{\perp}}{B_{\perp}^2 + \nu^2} - \frac{C_{\perp}}{C_{\perp}^2 + \nu^2} \right) (1 - \cos[(\Omega_1 - \Omega_2)\Delta z]) + \frac{C_{\perp}}{C_{\perp}^2 + \nu^2} \cdot \left(2 \frac{C_{\perp}}{C_{\perp}^2 + \nu^2} - \frac{A_{\perp}}{A_{\perp}^2 + \nu^2} \right. \\ &- \left. \left. \frac{B_{\perp}}{B_{\perp}^2 + \nu^2} \right) (1 - \cos[(\Omega_1 - \Omega_3)\Delta z]) + \frac{B_{\perp}}{B_{\perp}^2 + \nu^2} \cdot \frac{C_{\perp}}{C_{\perp}^2 + \nu^2} (1 - \cos[(\Omega_2 - \Omega_3)\Delta z]) \right. \\ &+ \frac{A_{\perp}}{A_{\perp}^2 + \nu^2} \cdot \left(\frac{D_{\perp}}{D_{\perp}^2 + \nu^2} - \frac{A_{\perp}}{A_{\perp}^2 + \nu^2} \right) (1 - \cos[\Omega_4\Delta z]) - \frac{A_{\perp}}{A_{\perp}^2 + \nu^2} \cdot \frac{D_{\perp}}{D_{\perp}^2 + \nu^2} (1 - \cos[\Omega_5\Delta z]) \\ &+ \left. \frac{1}{N_c^2} \frac{B_{\perp}}{B_{\perp}^2 + \nu^2} \cdot \left(\frac{A_{\perp}}{A_{\perp}^2 + \nu^2} - \frac{B_{\perp}}{B_{\perp}^2 + \nu^2} \right) (1 - \cos[(\Omega_1 - \Omega_2)\Delta z]) \right] \\ &+ \left. x^3 m^2 \left[\frac{1}{B_{\perp}^2 + \nu^2} \cdot \left(\frac{1}{B_{\perp}^2 + \nu^2} - \frac{1}{C_{\perp}^2 + \nu^2} \right) (1 - \cos[(\Omega_1 - \Omega_2)\Delta z]) + \dots \right] \right\} \quad (2.51) \end{aligned}$$

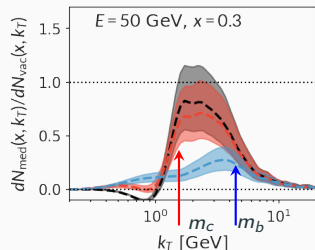
$$\begin{aligned} \left(\frac{dN^{\text{med}}}{dx d^2k_{\perp}} \right)_{g \rightarrow Q\bar{Q}} &= \frac{\alpha_s}{2\pi^2} T_R \int d\Delta z \frac{1}{\lambda_g(z)} \int d^2q_{\perp} \frac{1}{\sigma_{\text{el}}} \frac{d\sigma_{\text{el}}^{\text{med}}}{d^2q_{\perp}} \left\{ (x^2 + (1-x)^2) \right. \\ &\times \left[2 \frac{B_{\perp}}{B_{\perp}^2 + \nu^2} \cdot \left(\frac{B_{\perp}}{B_{\perp}^2 + \nu^2} - \frac{A_{\perp}}{A_{\perp}^2 + \nu^2} \right) (1 - \cos[(\Omega_1 - \Omega_2)\Delta z]) \right. \\ &+ 2 \frac{C_{\perp}}{C_{\perp}^2 + \nu^2} \cdot \left(\frac{C_{\perp}}{C_{\perp}^2 + \nu^2} - \frac{A_{\perp}}{A_{\perp}^2 + \nu^2} \right) (1 - \cos[(\Omega_1 - \Omega_3)\Delta z]) + \frac{1}{N_c^2 - 1} \left(2 \frac{B_{\perp}}{B_{\perp}^2 + \nu^2} \right. \\ &\times \left(\frac{C_{\perp}}{C_{\perp}^2 + \nu^2} - \frac{A_{\perp}}{A_{\perp}^2 + \nu^2} \right) (1 - \cos[(\Omega_1 - \Omega_2)\Delta z]) + 2 \frac{C_{\perp}}{C_{\perp}^2 + \nu^2} \cdot \left(\frac{B_{\perp}}{B_{\perp}^2 + \nu^2} - \frac{A_{\perp}}{A_{\perp}^2 + \nu^2} \right) \\ &\times (1 - \cos[(\Omega_1 - \Omega_3)\Delta z]) - 2 \frac{C_{\perp}}{C_{\perp}^2 + \nu^2} \cdot \frac{B_{\perp}}{B_{\perp}^2 + \nu^2} \cdot (1 - \cos[(\Omega_2 - \Omega_3)\Delta z]) \\ &+ 2 \frac{A_{\perp}}{A_{\perp}^2 + \nu^2} \cdot \left(\frac{A_{\perp}}{A_{\perp}^2 + \nu^2} - \frac{D_{\perp}}{D_{\perp}^2 + \nu^2} \right) (1 - \cos[\Omega_4\Delta z]) \\ &+ 2 \frac{A_{\perp}}{A_{\perp}^2 + \nu^2} \cdot \frac{D_{\perp}}{D_{\perp}^2 + \nu^2} (1 - \cos[\Omega_5\Delta z]) \left. \right] \\ &+ \left. m^2 \left[2 \frac{1}{B_{\perp}^2 + \nu^2} \cdot \left(\frac{1}{B_{\perp}^2 + \nu^2} - \frac{1}{A_{\perp}^2 + \nu^2} \right) (1 - \cos[(\Omega_1 - \Omega_2)\Delta z]) + \dots \right] \right\}. \quad (2.52) \end{aligned}$$

- Event-averaged $\frac{dN_{\text{med}}/dx/dk_{\perp}}{dN_{\text{vac}}/dx/dk_{\perp}} \triangleright$
Bands: $g_s = 1.8 \pm 0.2$.
- Mass effects modify radiation at finite x and $k_T \lesssim M$.

Pb-Pb, 5 TeV, 0-5%



Pb-Pb, 5 TeV, 0-5%

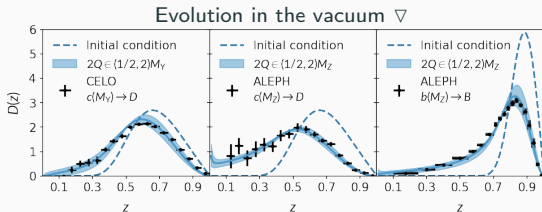


Fragmentation functions from the modified DGLAP evolution

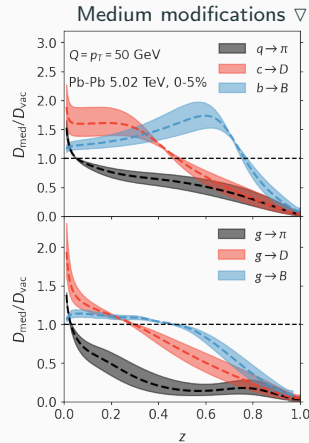
$$\frac{\partial D_{h/i}(z, Q^2)}{\partial \ln Q^2} = [P_{ji}^{\text{vac}} + \Delta P_{ji}^{\text{med}}] \otimes D_{h/j}(z, Q^2), \quad Q^2 = \frac{k_{\perp}^2 + xm_3^2 + (1-x)m_2^2 - x(1-x)m_1^2}{x(1-x)}$$

- Lund-Bowler initial condition ($Q_0 = 0.4 \text{ GeV}$) [Bowler ZPC11(1981)169] : $D_{D/c} = d(z, m_c)$, $D_{B/b} = d(z, m_b)$

$$d(z, m) = \frac{(1-z)^a}{z^{1+bm_T^2}} e^{-bm_T^2/z}, \quad a = 0.89, \quad b = 3.3 \text{ GeV}^2.$$

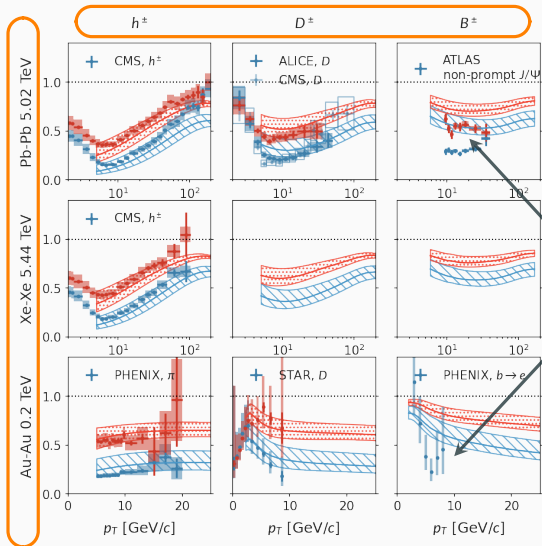


- $D_{D/g} = D_{B/g} = 0$ at $Q = Q_0$; non-zero but small at $Q > Q_0$ due to evolution. Non-perturbative input can be important for inclusive spectra [D. Anderle et al. PRD96(2017)034028] though not included.



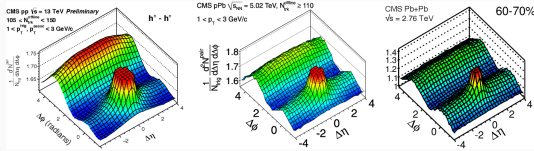
Inclusive spectra $d\sigma^i \sim q_T^{-N}$, $N \gg 1$
 $d\sigma^i \otimes D_{h/i}(z) \sim \int_{p_T/q_T}^1 z^{N-1} D(z) dz$

Nuclear modification factors in large colliding systems



- Jet-medium coupling constant $g_s = 1.8 \pm 0.2$ ($0.20 < \alpha_s < 0.32$).
- Reasonable description of R_{AA} for light and D (prefer slightly different g_s).
- Systematic deviations are more pronounced for B ($B \rightarrow J/\psi, e$) mesons.
 \Rightarrow possible missing physics:
 - Non-perturbative $g \rightarrow D, B$ input.
 - Interactions and break-up of heavy mesons in hadronic matter.

Identify QGP signals in small colliding system



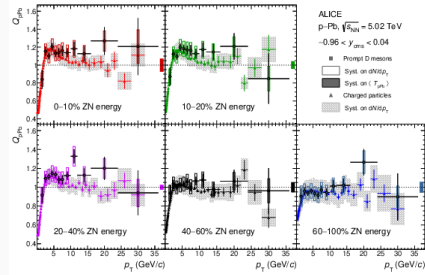
[CMS measured 2-particle correlations in p - p , p -Pb, Pb-Pb]

- Similarity between p -Pb and Pb-Pb can suggest final-state interactions in small systems.

T_{\max} [GeV] achieved in hydro simulation

p -Pb 5 TeV		O-O 7 TeV	
0-1%	60-90%	0-10%	30-50%
0.315	0.174	0.325	0.263

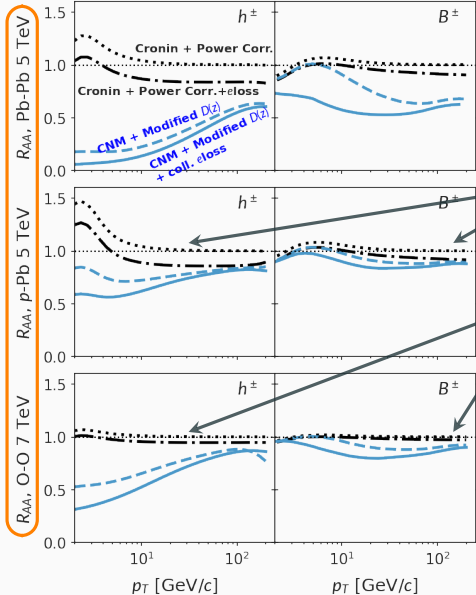
- But quenching of high- p_T hadrons and heavy flavors is not yet unambiguously observed.*



Δ D -meson $Q_{p\text{-Pb}}$, ALICE JHEP12(2019)092. Use neutrons in ZDC for centrality selection.

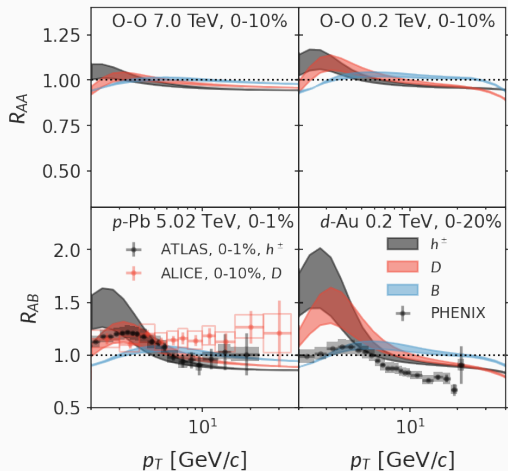
Need a better understanding of the baseline (no-QGP).

CNM and QGP effects small colliding systems



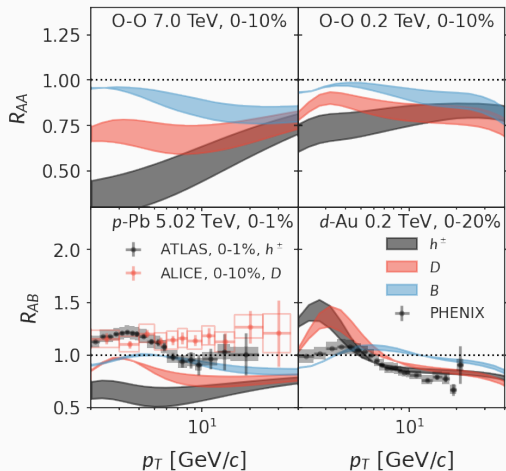
- Large A-A collisions: notable CNM effects but overwhelmed by energy loss in the QGP.
- Asymmetric p/d -A collisions: comparable CNM and QGP effects.
- Light A-A collisions: small CNM effects, good indicator of QGP effects in small systems.
- Relatively, collisional energy loss becomes important in small systems

Scenario I: no QGP formation, only cold nuclear matter effects



- d -Au data: [PHENIX, PRC96(2017)064905] ;
 p -Pb data: [ATLAS, PLB763(2016)313-336 (with $\langle T_{pA} \rangle$ calculated from the Glauber-Gribov model)] .
- CNM effects alone qualitatively describes h^\pm modifications in p -Pb, d -Au for $p_T > 5$ GeV.
- Cannot explain $R_{pA}^D > 1$ at high p_T .

Scenario II: with “QGP” formation



QGP in small systems created near T_c can be very different from large & high- T QGP.

In this special context, QGP color density is still assumed to be locally thermal $\propto T^3$ from hydro simulations.

- QGP effects in d -Au at $\sqrt{s} = 0.2$ TeV are small.
- For p -Pb at $\sqrt{s} = 5.02$ TeV, calculations with local-thermal QGP color density are inconsistent with data.
- To be tested by light-ion program at RHIC and LHC.

Medium-modified factorized calculation for HF with both IS and FS effects

- Initial-state broadening + dynamical shadowing + CNM energy loss.
- HTL collisional energy loss.
- Modified fragmentation evolved with SCET_G in-medium splitting functions.
- Ongoing efforts:
 - NP input to $g \rightarrow \text{HF mesons}$.
 - HF interactions in the hadronic phase.
 - Beyond CNM-eloss calculation, more sophisticated initial-state k_T -broadening.

Predictions of R_{AA} in small-system w/ and w/o QGP:

- CNM effects are strong in asymmetric small-large collisions (p -Pb and d -Au), weaker in O-O collisions.
- QGP corrections assuming local-thermal color density are inconsistent with R_{AA} in p -Pb.

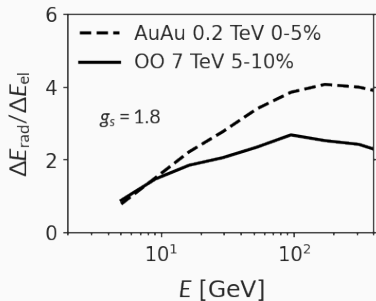
Questions?

Collisional energy loss in small systems

- Collisional and radiative energy loss scales different with medium geometry.
For example $T^3 \propto \tau^{-\alpha}$, neglecting logs in $\alpha_s, \ln(E/T), \dots$

$$\Delta E_{\text{rad}} \propto L^{2-\alpha} \quad \text{v.s.} \quad \Delta E_{\text{el}} \propto L^{1-\frac{2}{3}\alpha}$$

- From realistic hydro simulations of Au-Au 0.2 TeV 0-5% and O-O 7 TeV 5-10%
 - Similar initial temperature $T \approx 0.32$ GeV.
 - QGP size differ by a factor of 2.3.



- Define a “radiative energy loss”

$$\Delta E_{\text{rad}} = \int dk_{\perp}^2 \int_{1/2}^1 \frac{d\Delta P_{qq}^{\text{med}}}{dx dk_{\perp}^2} (1-x) dx$$

- Left: the relative importance of ΔE_{rad} (charm) is reduced relative to ΔE_{el} in the smaller system.